Heavy Water Models for Classical Molecular Dynamics: Effective Inclusion of Nuclear Quantum Effects

Victor Cruces Chamorro, Carmelo Tempra, and Pavel Jungwirth*

Institute of Organic Chemistry and Biochemistry of the Czech Academy of Sciences, Flemingovo nám. 542/2, 160 00 Prague 6, Czech Republic

E-mail: pavel.jungwirth@uochb.cas.cz

April 14, 2021

Abstract

Small differences in physical and chemical properties of H_2O and D_2O, such as melting and boiling points or pKa, can be traced back a slightly stronger hydrogen bonding in heavy versus normal water. In particular, deuteration reduces zero-point vibrational energies as a demonstration of nuclear quantum effects. In principle, computationally demanding quantum molecular dynamics is required to model such effects. However, as already demonstrated by Feynmann and Hibbs, zero point vibrations can be effectively accounted for by modifying the interaction potential within classical dynamics. In the spirit of the Feymann-Hibbs approach, we develop here two water models for classical molecular dynamics by fitting experimental differences between H_2O and D_2O. We show that a 3-site SPCE-based model accurately reproduces differences between properties of the two water isotopes, with a 4-site TIP4P-2005/based model in addition capturing also the absolute values of key properties of heavy water. The present models are computationally simple enough to allow for extensive simulations of biomolecules in heavy water relevant, e.g., for experimental techniques such as NMR or neutron scattering.

Introduction

Substitution of hydrogen by deuterium in water leads not only to a $\sim$10 % higher mass density primarily due to the doubled mass of the latter isotope, but also to small shifts in other observable properties such as the temperature of maximum density (TMD), melting point, self-diffusion coefficient, viscosity, etc[1–3]. The origins of these differences between ordinary water (H_2O) and heavy water (D_2O) are due to nuclear quantum effects (NQEs), which can also be invoked to rationalize why the number density (i.e., the number of molecules per unit volume) of D_2O water is slightly smaller than that of H_2O. Typically, the isotopic effect becomes more pronounced if proton or deuteron chemically detaches, such as during proton

transfer processes. Nevertheless, while pH of ordinary water at 25 ^{o}C is 7.0, pD of heavy water is not very different, reaching 7.44. Finally, note that due to the fact that NQEs are typically larger for lighter particles, they tend to be more pronounced in H_2O than in D_2O.

The above differences between ordinary and heavy water, in particular kinetic effects concerning proton/deuteron transfer, are behind the very low toxicity of D_2O to higher organisms, which only becomes an issue if a sizable amount (tens of percent) of bodily water is replaced by its deuterated analogue[4,5]. On a safer note, we have recently confirmed old claims that heavy water has mildly but distinctly sweet taste, showing that D_2O (unlike H_2O) activated the human sweet taste receptor[6]. While the exact molecular mechanism of the sweet taste of D_2O remains elusive, our simulations confirm experimental observations that in general protein stability and rigidity changes (typically slightly increases) upon moving from ordinary to heavy water[7–9].

Changes in protein behavior in ordinary vs. heavy water are primarily due to differences in hydrogen bonding due to NQEs[3]. Namely, a reduction in vibrational zero point energies leads to slightly stronger water-water and water-protein hydrogen bonds in D_2O vs H_2O[3]. Molecular simulations should be able to shed light on this phenomenon. However, for description of NQEs one should in principle employ quantum approaches such as the path integral molecular dynamics. While applicable nowadays to small unit cells of water or simple aqueous solutions[10–12], the path integral approach is hardly computationally feasible for large systems involving proteins and other biomolecules in aqueous environments.

Feymann and Hibbs[13] suggested to simplify the path integral theory using a harmonic approximation, which results in a modification of the interaction potential within classical molecular dynamics (MD)[14,15]. In the spirit of this approach, we develop here effective 3-site and 4-site heavy water models for classical MD that allow for accurate and at the same time

computationally efficient modelling of biomolecules in D_2O, as encountered, e.g., in NMR and neutron scattering experiments. Following a previous attempt in this direction[16] and parallel to the most recent approach involving an adaptive quantum thermal bath[17], the present heavy water models are demonstrated to be capable to recover quantitatively the key experimental differences between ordinary and heavy water.

Methods

Effective inclusion of zero point energy effects, which are behind differences between properties of D_2O and H_2O, is realized by tuning the interaction potential to reproduce experimental observables that exhibit the strongest NQEs. A proper choice of such target observables is essential for the best possible performance of the developed empirical water models[18,19], in particular when the optimized parameter set is limited. For common water parameterizations, where the intermolecular potential contains Lennard-Jones and electrostatic terms, the number of the corresponding adjustable parameters is small, i.e., four for the 4-site TIP4P-2005 model[20] or three for the 3-site SPC/E model[21]. The number of adjustable parameters then dictates the minimal number of target experimental observables.

Table 1: Target properties used in this study, i.e., density at ambient conditions, temperature of maximum density (TMD), self-diffusion coefficient D_{OW}, and viscosity (η), and.

Property	Expt. LW	Expt. HW	Exp. Shift
density[kg/m^3]	997.05	1104.40	107.35
TMD[K]	277.13	284.34	7.21
D_{OW}[cm^{-2}s]	2.30	1.77	-23.04%
η[mPa·s]	0.890	1.097	23.26%

Here, we chose as target properties the following four experimental observables of D_2O and H_2O - density at ambient conditions, TMD, self-diffusion coefficient, and viscosity (Table 1). Note that the last two properties are strictly speaking not independent as they can

be under certain assumptions related to each other via the Stokes-Einstein relation[22]. As a consequence, for the 4-site model we constrained the dipole moment of the heavy water model to that of the reference water model.

Viscosity was calculated using Green-Kubo equation[22,23]

$$\eta = \frac{V}{k_B T} \int_0^\infty \langle P_{\alpha\beta}(t) P_{\alpha\beta}(t_0) \rangle dt \tag{1}$$

where V is the simulation volume, and $P_{\alpha\beta}$ are the off-diagonal terms of the pressure tensor. We reduced the statistical error by averaging over 20 ns-long autocorrelation functions of the off-diagonal pressure tensor for the whole NVT simulation[24,25].

For calculation of surface tension[26], we elongated the unit cell size along the z-axis and run simulations at a constant volume. In this way, we ensure that a slab of water is formed with a sufficiently wide vacuum layer separating it from its periodic images. The surface tension of planar interfaces can be calculated from the asymmetry of the pressure tensor

$$\gamma = \frac{L_z}{2} \left[P_{zz} - \left(\frac{P_{xx} + P_{yy}}{2} \right) \right] \tag{2}$$

where P_{zz} is the normal component of the pressure tensor and P_{xx} and P_{yy} are the tangential components. Note that we use the average of the two tangential components to reduce the statistical error.

The functional forms of the reference water models, i.e., the 4-site TIP4P-2005[20] and the 3-site SPC/E[21], are similar to each other with both having partial charges on hydrogen atoms and with only the oxygen atom carrying Lennard-Jones parameters. The differences between the two models are in the molecular geometry and the position of the negative charge, which for SPC/E is located at the oxygen atom while for TIP4P-2005 it is placed

Table 2: Potential parameters of 4-site models, i.e, TIP4P-2005 for ordinary water and (newly developed) TIP4P-HW for heavy water

Parameters	TIP4P-2005[20]	TIP4P-HW
d_{OH}/nm	0.09572	0.09572
α_{HOH}/deg	104.52	104.52
σ/nm	0.31589	0.31658
ϵ/(kJ/mol)	0.7749	0.7330
q_{H}/au	0.5564	0.55705
d_{OM}/nm	0.01546	0.01551

at an additional virtual atom site at the HOH angle bisector. The potential parameters of these water models, together with those of the existing[16] and here developed D_2O models are summarized in Tables 2 and 3.

Table 3: Potential parameters of 3-site models, i.e, SPC/E[21] for ordinary water, as well as an existing SPC/HW[16] and here developed SPCE-HW parameterizations for heavy water

Parameters	SPC/E[21]	SPCE-HW	SPC/HW[16]
d_{OH}/nm	0.10000	0.10000	0.10000
α_{HOH}/deg	109.47	109.47	109.47
σ/nm	0.31657	0.31970	0.31658
ϵ/(kJ/mol)	0.6502	0.5050	0.6497
q_{H}/au	0.4238	0.4188	0.4350

For molecular dynamics simulations of 1110 water molecules in the unit cell we employed either the isothermal-isobaric ensemble (NpT) or the canonical ensemble (NVT), where the volume used in the later ensemble was the average volume of the NpT simulations, with the only exception of surface tension calculations that were performances with the z-axis elongated to 17.5 nm. Temperature was kept constant at 298 K using the Noosé-Hoover thermostat[27] with a time coupling constant of 1ps. For the NpT ensemble, pressure was set at 1 bar using the Parrinello-Rahman barostat[28] with a time coupling constant of 2.5 ps, and a compressibility of $5 \cdot 10^{-5}$ bar^{-1}. A cut-off radius of 1.2 nm was complemented with the

particle-mesh Edwald procedure[29] to account for long-range interactions. Additional cut-off schemes were tested as described in detail in the Supporting Information (SI). Finally, the water molecular geometry was fixed with LINCS algorithm[30], which allowed for the use of a time step of 2 fs for the production runs of at least 50 ns. All simulations were performed using GROMACS 2019.4[31] package.

Results and Discussion

The performance of the newly developed heavy water models, together with that of the original ordinary water models, with respect to the selected key experimental observables is presented in Tables 4 and 5. Namely, Table 4 summarizes the results for the 4-site TIP4P-HW model, while Table 5 analogously shows values for the 3-site SPCE-HW parameterization. For comparison, the later table also provides analogous results for the previously developed SPC/HW model[16]. We see from Table 4 that our TIP4P-HW model reproduces D_2O thermodynamic properties with comparable accuracy as does TIP4P-2005 for H_2O. Importantly, TIP4P-HW compares quantitatively to experiment not only for the target properties but also for additional thermodynamic observables such as the isothermal compressibility, isobaric thermal expansivity, and surface tension (Table 4). A notable exception is the underestimated dielectric constant for both D_2O and H_2O, which is a common artifact of many non-polarizable water models that do not explicitly account for electronic polarization[19].

For SPCE-HW the situation is different. As the original SPC/E model for H_2O is rather inaccurate in predicting important points at the phase diagram such as the melting temperature or TMD[19], one can hardly expect from SPCE-HW an absolute accuracy in these properties for D_2O. Nevertheless, as demonstrated in Table 5 the SPCE-HW model quantitatively reproduces experimental H_2O-to-D_2O shifts for all the monitored observables. This represents a major improvement in comparison to the previously developed SPC/HW model

which dramatically overestimates in absolute values these shifts for practically all the observables (see Table 5).

As of dynamic properties, we start with the self-diffusion coefficient which can be calculated simply from mean square displacements (MSD)[22]. The simulated self-diffusion coefficients for TIP4P-HW and SPCE-HW, presented in Tables 4 and 5, demonstrate that the resulting picture is the same as for thermodynamic properties. Namely, the 4-site model reproduces the experimental observable in absolute terms, while the 3-site model at least recovers the D_2O vs H_2O difference. The same is true for also for viscosity (see Tables 4 and 5).

Table 4: Simulation results of TIP4P-2005[20] and TIP4P-HW as compared to experiment for the target properties - density, TMD, self-diffusion coefficient, and viscosity, as well as for isothermal compressibility, isobaric thermal expansivity, surface tension, and dielectric constant. Simulations were performed at 298 K and 1 bar.

Property	TIP4P-2005[20]	H_2O Expt.	TIP4P-HW	D_2O Expt.
density[kg/m^3]	997.2	997.05	1104.4	1104.4
TMD[K]	277	277.13	283	284.34
D_{OW}[cm^{-2}s]	2.10	2.30	1.69	1.77
η[mPa·s]	0.86	0.89	1.05	1.10
$\kappa_T[10^{-6}$/bar]	49.2	45.248	50.0	46.53
$\alpha_p[10^{-4}$/K]	3.0	2.57	2.5	1.91
γ[mN/m]	69.2	71.98	68.6	71.87
ϵ_r	58	78.4	57	78.1

On top of the observables presented in Tables 4 and 5 we also checked how well our models reproduce heavy water density in the range of temperature corresponding to a liquid, as well as for a wide range of pressures from 1 to 1000 bar (Figure 1). It is worth mentioning that in the whole range of explored temperatures and pressures the D_2O density is lower than that of H_2O multiplied by the D_2O/H_2O mass ratio of 1.1114 (see Figure 1). This is a clear demonstration of the slightly stronger hydrogen bonding in D_2O due to NQEs, which makes heavy water a bit more "ice-like" and, therefore, less dense in terms of molecular

Table 5: Simulation results of SPC/E[21], SPC/HW[16], and SPCE-HW. Comparison to experiment is made for H_2O-to-D_2O shifts (these shifts for the two models and for experimental values are denoted as Δ in the table) of the target properties - density, TMD, self-diffusion coefficient, and viscosity, as well as of isothermal compressibility, isobaric thermal expansivity, surface tension, and dielectric constant. Simulations were performed at 298 K and 1 bar.

Poperty	SPC/E[21]	SPCE-HW	$\Delta_{\text{SPCE-HW}}$	SPC/HW[16]	$\Delta_{\text{SPC/HW}}$	Δ_{Expt}
Density[kg/m^3]	999.2	1103.0	103.8	1125.4	126.2	107.3
TMD[K]	249	250	1.0	269	20	7.21
DD_{OW}[cm^{-2}s]	2.50	1.95	-22.0%	1.35	-85.2%	-23.26%
η[mPa·s]	0.73	0.88	20.5%	1.42	94.2%	23.04%
$\kappa_T[10^{-6}/\text{bar}]$	50.4	50.3	-0.1	44.4	-6.0	1.282
$\alpha_p[10^{-4}/\text{K}]$	4.8	5.1	0.3	4.4	-0.4	-0.66
γ[mN/m]	62.2	57.5	-4.7	68.8	6.6	-0.09
ϵ_r	70	67	-3.0	76	6.0	-0.3

number density than ordinary water.

We see from Figure 1 A,B that the TIP4P-HW model quantitatively recovers the experimental non-monotonous dependence of D_2O density on temperature, as well as the linear dependence on pressure, with the same (if not better) accuracy as TIP4P-2005 does for H_2O. While the pressure dependence of D_2O or H_2O density at room temperature is almost quantitatively reproduced also for the SPCE-HW or SPC/E models, the temperature dependencies are only qualitatively described being shifted down by about 30 K compared to the experiment for both systems (figure 1) C,D. Note that the older SPC/HW model[16] performs poorly, missing on both the temperature and pressure density dependencies (Figure 1 C,D).

Next, in Figures 2 and 3 we present the oxygen-oxygen radial distribution functions (RDF), as well as the corresponding structure factors in the reciprocal space (as directly measured, e.g., by X-ray[32] or neutron scattering[33]). We see that both the 4-site and 3-site water models agree semi-quantitatively with experiment; nevertheless the residual errors are larger than the tiny difference between the RDFs of D_2O and H_2O[34].

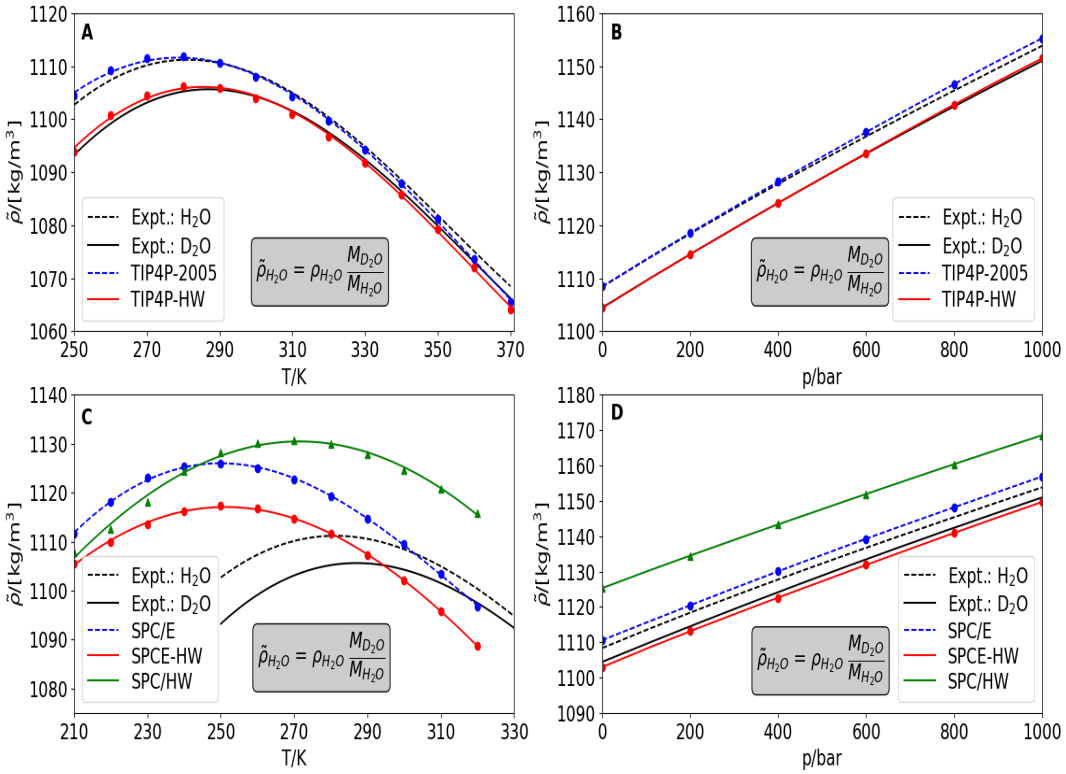

Figure 1: Densities of heavy and ordinary water as functions of temperature at 1 bar (A and C) and pressure at 298 K (B and D) for the 4-site (A and B) and 3-site (C and D) water models, as compared to experimental values (in black). Note that the ordinary water density is rescaled by the D_2O/H_2O mass ratio.

Overall, the present heavy water models, albeit simple and computationally cheap, account effectively but quantitatively for the experimental differences between D_2O or H_2O due to NQEs both in thermodynamic and dynamic properties. The 4-site TIP4P-HW D_2O model built on the very accurate TIP4P-2005 H_2O parameterization reproduces also heavy water properties in absolute terms. This cannot be expected from SPCE-HW based on a (in many respects) rather inaccurate 3-site SPC/E model[18,19], nevertheless, it performs significantly better than the earlier developed SPC/HW D_2O parameterization[16]. The principal differences between the present SPCE-HW model and the older SPCE/HW one[16] stem from

the choice of parameters for optimization and selection of target properties. Here, we picked a wider range of properties directly reflecting NQEs and chose to re-adjust the Lennard-Jones parameters on top of fitting partial charges.

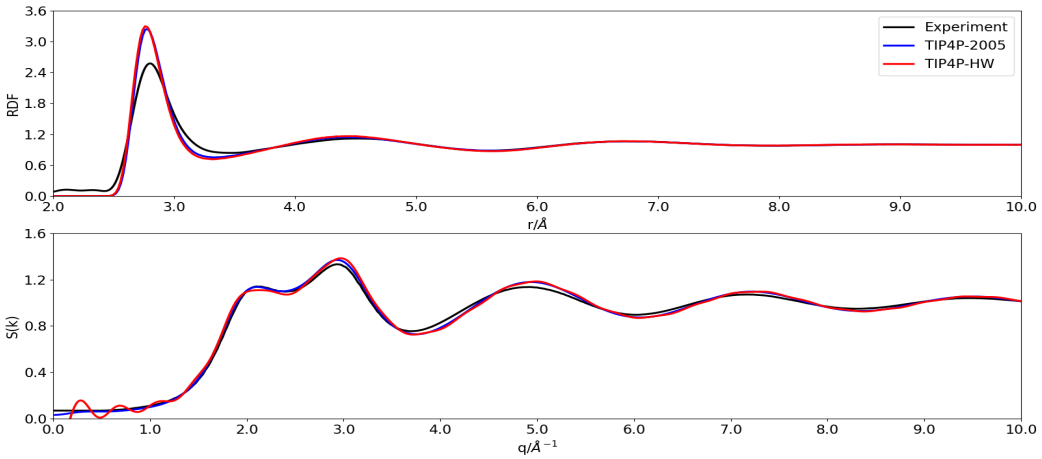

Figure 2: Radial distribution functions (top) and the corresponding structure factors (bottom) of TIP4P-2005[20] and TIP4P-HW at 298 K and 1 bar. The experimental result (black

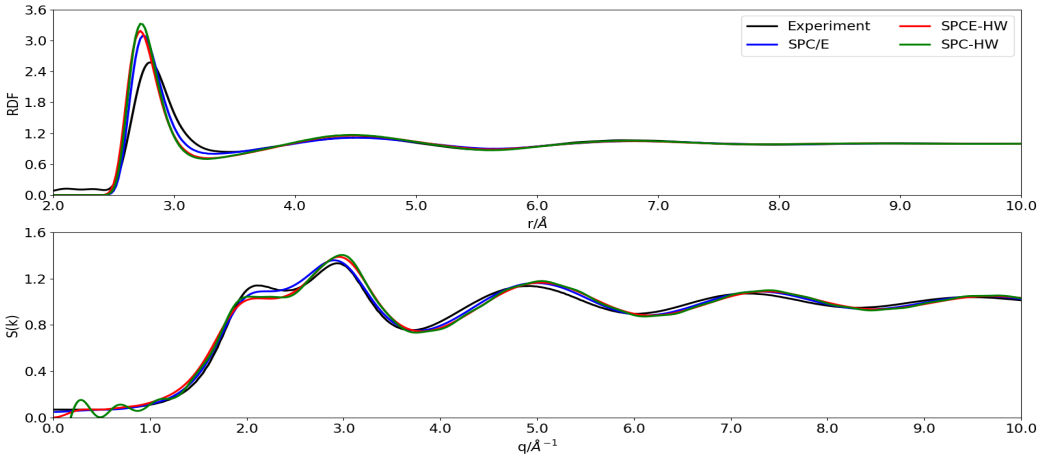

Figure 3: Radial distribution functions (top) and the corresponding structure factors (bottom) of SPC/E[21], SPC/HW[16], and SPCE-HW at 298 K and 1 bar. The experimental result (black line) was obtained from Reference[32]

.

Conclusions

Based on existing 4-site TIP4P-2005 and 3-site SPC/E ordinary water models we have developed here the corresponding two models for heavy water. In the spirit of the formalism by Feynmann and Hibbs[13] we have accounted for nuclear quantum effects by effectively incorporating them into the interaction potential within classical force field molecular dynamics. We have demonstrated that such an approach is capable for capturing differences between ordinary and heavy water with the 4-site model being also able to reproduce absolute values of key thermodynamic and dynamic observables for D_2O. With no extra computational overhead compared to standard classical molecular dynamics simulations the present approach opens the possibility to investigate nuclear quantum effects on dissolved biomolecules connected with water deuteration, as encountered for example within NMR or neutron scattering experiments.

Associated Content

Supporting Information

The Supporting Information is available free of charge on the ACS Publications website. It contains primarily a detailed description of various cut-off schemes for intermolecular potentials and their effect within the simulations on the experimental observables.

Acknowledgement

V.C.C. and C.T. acknowledge support from the Charles University in Prague and from the International Max Planck Research School in Dresden. All authors acknowledge support from the Czech Science Foundation via EXPRO Grant no. 19-26854X. Computational resources were supplied by the project "e-Infrastruktura CZ" (e-INFRA LM2018140) provided within

the program Projects of Large Research, Development and Innovations Infrastructures.

References

(1) Hill, P. G.; MacMillan, R. D. C.; Lee, V. A Fundamental Equation of State for Heavy Water. *Journal of Physical and Chemical Reference Data* **1982**, *11*, 1–14.

(2) Blahut, A.; Hykl, J.; Peukert, P.; Vinš, V.; Hrubý, J. Relative density and isobaric expansivity of cold and supercooled heavy water from 254 to 298 K and up to 100 MPa. *The Journal of Chemical Physics* **2019**, *151*, 034505.

(3) Ceriotti, M.; Fang, W.; Kusalik, P. G.; McKenzie, R. H.; Michaelides, A.; Morales, M. A.; Markland, T. E. Nuclear Quantum Effects in Water and Aqueous Systems: Experiment, Theory, and Current Challenges. *Chemical Reviews* **2016**, *116*, 7529–7550.

(4) Barbour, H. G. The Basis of the Pharmacological Action of Heavy Water in Mammals. *The Yale journal of biology and medicine* **1937**, *9*, 551–65.

(5) Siegel, S. M.; Galun, E. Differential effects of deuterium oxide on the growth and morphogenesis of Trichoderma viride. *Plant and Cell Physiology* **1978**, *19*, 851–856.

(6) Abu, N. B.; Mason, P. E.; Klein, H.; Dubovski, N.; Shoshan-Galeczki, Y. B.; Malach, E.; Pražienková, V.; Maletínská, L.; Tempra, C.; Chamorro, V. C. et al. Sweet taste of heavy water. *Communications Biology* **2021**, *4*, 2399–3642.

(7) Sasisanker, P.; Oleinikova, A.; Weingärtner, H.; Ravindra, R.; Winter, R. Solvation properties and stability of ribonuclease A in normal and deuterated water studied by dielectric relaxation and differential scanning/pressure perturbation calorimetry. *Phys. Chem. Chem. Phys.* **2004**, *6*, 1899–1905.

(8) Efimova, Y. M.; Haemers, S.; Wierczinski, B.; Norde, W.; Well, A. A. v. Stability of globular proteins in H2O and D2O. *Biopolymers* **2007**, *85*, 264–273.

(9) Cioni, P.; Strambini, G. B. Effect of Heavy Water on Protein Flexibility. *Biophysical Journal* **2002**, *82*, 3246 – 3253.

(10) Habershon, S.; Markland, T. E.; Manolopoulos, D. E. Competing quantum effects in the dynamics of a flexible water model. *The Journal of Chemical Physics* **2009**, *131*, 024501.

(11) McBride, C.; Aragones, J. L.; Noya, E. G.; Vega, C. A study of the influence of isotopic substitution on the melting point and temperature of maximum density of water by means of path integral simulations of rigid models. *Phys. Chem. Chem. Phys.* **2012**, *14*, 15199–15205.

(12) McBride, C.; Noya, E. G.; Aragones, J. L.; Conde, M. M.; Vega, C. The phase diagram of water from quantum simulations. *Phys. Chem. Chem. Phys.* **2012**, *14*, 10140–10146.

(13) Feynman, R. P.; Hibbs, A. *Quantum Mechanics and Path Integrals*; McGraw-Hill: New York, 1965.

(14) Sesé, L. M. Feynman-Hibbs quantum effective potentials for Monte Carlo simulations of liquid neon. *Molecular Physics* **1993**, *78*, 1167–1177.

(15) Slavíček, P.; Jungwirth, P.; Lewerenz, M.; Nahler, N. H.; Fárník, M.; Buck, U. Pickup and Photodissociation of Hydrogen Halides in Floppy Neon Clusters. *The Journal of Physical Chemistry A* **2003**, *107*, 7743–7754.

(16) Grigera, J. R. An effective pair potential for heavy water. *The Journal of Chemical Physics* **2001**, *114*, 8064–8067.

(17) Mauger, N.; Plé, T.; Lagardère, L.; Bonella, S.; Mangaud, E.; Piquemal, J.-P.; Huppert, S. Nuclear Quantum Effects in liquid water at near classical computational cost using the adaptive Quantum Thermal Bath. 2021.

(18) Guillot, B. A reappraisal of what we have learnt during three decades of computer simulations on water. *Journal of Molecular Liquids* **2002**, *101*, 219–260.

(19) Vega, C.; Abascal, J. L. F. Simulating water with rigid non-polarizable models: a general perspective. *Phys. Chem. Chem. Phys.* **2011**, *13*, 19663–19688.

(20) Abascal, J. L. F.; Vega, C. A general purpose model for the condensed phases of water: TIP4P/2005. *The Journal of Chemical Physics* **2005**, *123*, 234505.

(21) Berendsen, H. J. C.; Grigera, J. R.; Straatsma, T. P. The missing term in effective pair potentials. *The Journal of Physical Chemistry* **1987**, *91*, 6269–6271.

(22) Allen, M. P.; Tildsley, D. J. *Computer Simulation of Liquids, Ed. 1*; Oxford Sience Publications: Oxford, 1987.

(23) McQuarrie, D. A. *Statistical Mechanics*; University Science Books: California, 2000.

(24) González, M. A.; Abascal, J. L. F. The shear viscosity of rigid water models. *The Journal of Chemical Physics* **2010**, *132*, 096101.

(25) Hess, B. Determining the shear viscosity of model liquids from molecular dynamics simulations. *The Journal of Chemical Physics* **2002**, *116*, 209–217.

(26) Sega, M.; Dellago, C. Long-Range Dispersion Effects on the Water/Vapor Interface Simulated Using the Most Common Models. *The Journal of Physical Chemistry B* **2017**, *121*, 3798–3803.

(27) Hoover, W. G. Canonical dynamics: Equilibrium phase-space distributions. *Phys. Rev. A* **1985**, *31*, 1695–1697.

(28) Parrinello, M.; Rahman, A. Polymorphic transitions in single crystals: A new molecular dynamics method. *Journal of Applied Physics* **1981**, *52*, 7182–7190.

(29) Essmann, U.; Perera, L.; Berkowitz, M. L.; Darden, T.; Lee, H.; Pedersen, L. G. A smooth particle mesh Ewald method. *The Journal of Chemical Physics* **1995**, *103*, 8577–8593.

(30) Hess, B.; Bekker, H.; Berendsen, H. J. C.; Fraaije, J. G. E. M. LINCS: A linear constraint solver for molecular simulations. *Journal of Computational Chemistry* **1997**, *18*, 1463–1472.

(31) Abraham, M. J.; Murtola, T.; Schulz, R.; Páll, S.; Smith, J. C.; Hess, B.; Lindahl, E. GROMACS: High performance molecular simulations through multi-level parallelism from laptops to supercomputers. *SoftwareX* **2015**, *1-2*, 19–25.

(32) Skinner, L. B.; Huang, C.; Schlesinger, D.; Pettersson, L. G. M.; Nilsson, A.; Benmore, C. J. Benchmark oxygen-oxygen pair-distribution function of ambient water from x-ray diffraction measurements with a wide Q-range. *The Journal of Chemical Physics* **2013**, *138*, 074506.

(33) Head-Gordon, T.; Hura, G. Water Structure from Scattering Experiments and Simulation. *Chemical Reviews* **2002**, *102*, 2651–2670.

(34) Paesani, F.; Voth, G. A. The Properties of Water: Insights from Quantum Simulations. *The Journal of Physical Chemistry B* **2009**, *113*, 5702–5719.

For Table of Contents Only